

ESTIMATION OF BINDING ENERGY OF XI-MINUS HYPERON IN A NUCLEUS FROM SINGLE- Λ HYPERNUCLEUS EVENT

Khin Than Tint¹, Aye Moh Moh Myo², Yi Yi Myint³, K. Nakazawa⁴

Abstract

The binding energy of Xi-minus (Ξ^-) hyperon in nitrogen nucleus was estimated from single- Λ hypernucleus event which was detected in nuclear emulsion of J-ARC E07 experiment. The type of hypernucleus, its production and decay mode were obtained based on the conservation laws of energy and momentum. Moreover, the estimated value of the binding energy of Ξ^- hyperon in nitrogen nucleus was 0.51 ± 0.17 MeV.

Keywords: Xi-minus hyperon, binding energy, single- Λ hypernucleus event, nuclear emulsion

Introduction

Ξ^- hyperons were produced via the (K^- , K^+) reaction in a diamond target with the momentum of the K^- meson beam, 1.81 GeV/c in J-PARC E07 experiment. The Ξ^- hyperons were captured by nuclei in nuclear emulsion and become compound nuclei with $S = -2$. At the decay of compound Ξ^- nuclei, single- Λ hypernucleus, twin single- Λ hypernuclei, double Λ hypernucleus can be emitted. The binding energy of Ξ^- hyperon in a nucleus can be obtained more exactly from twin single- Λ hypernuclei event. In the twin single- Λ hypernuclei event, two single- Λ hypernuclei were emitted back to back from the stopping point of Ξ^- hyperons. The kinetic energy and momentum of two single- Λ hypernuclei can be obtained from their range. The binding energy of Ξ^- hyperon can be obtained from the momentum balance of two single- Λ hypernuclei. On the other hand, one single- Λ hypernucleus track and Λ hyperon (invisible in nuclear emulsion) were emitted at the stopping point of Ξ^- hyperon, i.e decay point of Ξ^- nucleus in single- Λ hypernucleus event. In this case, the energy and momentum of the single- Λ hypernucleus can be measured from its range. However, the energy and momentum of Λ hyperon cannot determine exactly due to invisible in nuclear emulsion. In this analysis, binding energy of Ξ^- hyperons in nitrogen nucleus is obtained from, the difference between Q value and total energy (single- Λ hypernucleus + invisible Λ hyperon).

Event Analysis

Event Description of A Single- Λ hypernucleus Event

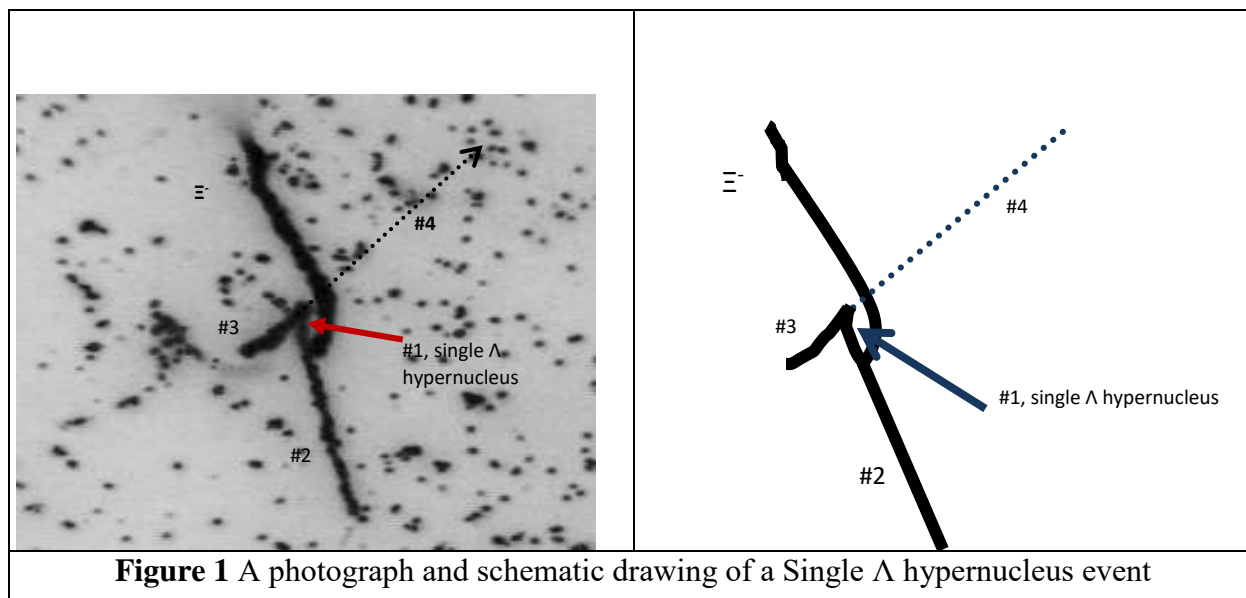
The single- Λ hypernucleus event was detected at up-stream of Module #26, plate #5. Figure 1 shows a photograph and a schematic drawing of the single- Λ hypernucleus event. The Ξ^- hyperon came to rest at vertex A, where two charged particle tracks (track #1, track #2) and uncharged particle track (invisible) Λ hyperon were emitted. The particle of track #1 decayed into a π^- meson (track #4) and other charged particle (track #3) at point B. Hence, #1 was identified as a single- Λ hypernucleus. The end of tracks #2, #3 were traced manually and found the stopping points in the same layer of nuclear emulsion. Track #4 (thin track) was passed through the upper layer of emulsion plate # 5 and stopped in plate # 2.

¹ Dr, Associate Professor, Department of Physics, University of Mandalay

² MSc, Department of Physics, Yadanabon University

³ Dr, Professor and head, Department of Physics, Yadanabon University

⁴ Dr, Senior Professor, Department of Physics, Gifu University, Japan.



Range and Angle Measurement

We measured the ranges and emission angles of the tracks from single- Λ hypernucleus event by using the microscope system. The range of the tracks, R , can be obtained from measured (x, y, z) coordinates of tracks by using the following equation,

$$R = \sqrt{\Delta X^2 + \Delta Y^2 + (\Delta Z \times S)^2} \quad (1)$$

where, ΔX , ΔY and ΔZ as the length in the x , y and z direction respectively. The shrinkage factor of dried emulsion, S , is defined by the ratio of the thickness of the emulsion plate at the time of beam exposure and measurement. The zenith angle (θ) and azimuthal angle (ϕ) of each track were obtained from the coordinates at vertex and suitable clicked point on the track.

Range-Energy Relation Calibration in Nuclear Emulsion

The observable things in nuclear emulsion were ranges, angles, and a grain density of charge particle tracks. In order to calculate the masses of hypernuclei, the energy of the decay daughters was necessary. The kinetic energy of a charged particle is provided by measuring the range if we assume the nuclear species. The range-energy relation is essential for emulsion analysis.

The alpha decays which have topologies of Thorium series were used as range energy calibration source. Total 57 events have straight and long range track, alpha particle decays from ^{212}Po , were used. The method of range-energy relation calibration or the estimation of density nuclear emulsion plate was already described elsewhere. The density and Shrinkage factor of an emulsion plate of Pl#5, Mod #26 were $3.59 \pm 0.02 \text{ gcm}^{-3}$ and 2.2 ± 0.01 , respectively.

Event Reconstruction

The event construction in nuclear emulsion was based on the conservation laws of energy and momentum. The kinetic energies of the charged particles were calculated from their range by means of a range-energy relation and for neutral particles it was calculated from the momentum balance. The errors of kinetic energy come from the errors of range. On the other hand, the errors of total energy come from the errors of range, angles and rest mass.

Firstly, we considered that the Ξ^- hyperon was absorbed by a light nucleus (C, N, and O) in nuclear emulsion at the point A. Since the length of track #1 is as short as $3.3 \pm 0.2 \mu\text{m}$, the Ξ^- hyperon was assumed to be captured in a light nucleus. In nuclear emulsion at point A from which single Λ hypernucleus (track #1), track #2 and invisible Λ hyperon were emitted. The Q value, the total kinetic energy of emitted particles (E_{Total}) were calculated and compared. Table (1), Table (2), Table (3) and Table (4) summarized the some possible production reaction modes from $\Xi^- + {}^6_{12}\text{C}$, ${}^7_{14}\text{N}$, ${}^8_{16}\text{O}$ to a Λ hyper nucleus (track #1, track #2) and invisible Λ hyperon.

Table 1 Some production reaction modes of the single Λ hypernucleus without neutron emission.

Possible Production Reaction	Q-value (MeV)	E_{total} (MeV)	B_{Ξ^-} (MeV) = $Q - E_{\text{Total}}$
$\Xi^- + {}^{14}_7\text{N} \rightarrow {}^{10}_{\Lambda}\text{Be} + {}^4\text{He} + \Lambda^0$	19.01	18.51 ± 0.17	0.51 ± 0.17
$\Xi^- + {}^{12}_6\text{C} \rightarrow {}^8_{\Lambda}\text{Li} + {}^4\text{He} + \Lambda^0$	10.78	14.45 ± 0.14	-3.66 ± 0.14
$\Xi^- + {}^{13}_6\text{C} \rightarrow {}^9_{\Lambda}\text{Li} + {}^4\text{He} + \Lambda^0$	9.57	14.66 ± 0.14	-5.09 ± 0.14
$\Xi^- + {}^{12}_6\text{C} \rightarrow {}^9_{\Lambda}\text{Be} + {}^3\text{H} + \Lambda^0$	8.14	24.75 ± 0.17	-6.66 ± 0.17
$\Xi^- + {}^{16}_8\text{O} \rightarrow {}^{12}_{\Lambda}\text{B} + {}^4\text{He} + \Lambda^0$	16.86	25.07 ± 0.22	-8.21 ± 0.22
$\Xi^- + {}^{13}_7\text{C} \rightarrow {}^{10}_{\Lambda}\text{Be} + {}^3\text{H} + \Lambda^0$	7.26	15.73 ± 0.16	-8.47 ± 0.16
$\Xi^- + {}^{17}_8\text{O} \rightarrow {}^{13}_{\Lambda}\text{B} + {}^4\text{He} + \Lambda^0$	17.20	26.20 ± 0.22	-8.99 ± 0.22
$\Xi^- + {}^{12}_6\text{C} \rightarrow {}^{10}_{\Lambda}\text{Be} + {}^2\text{H} + \Lambda^0$	5.45	16.42 ± 0.16	-10.48 ± 0.16
$\Xi^- + {}^{14}_7\text{N} \rightarrow {}^{12}_{\Lambda}\text{B} + {}^2\text{H} + \Lambda^0$	13.75	25.895 ± 0.21	-12.15 ± 0.21
$\Xi^- + {}^{14}_7\text{N} \rightarrow {}^{13}_{\Lambda}\text{B} + {}^1\text{H} + \Lambda^0$	16.01	29.633 ± 0.20	-13.63 ± 0.20

Table 2 Some production reaction modes of the single Λ hypernucleus with one neutron emission

Possible Production Reaction	Q-Value (MeV)	E_{total} (MeV)	B_{Ξ} (MeV) = $Q - E_{\text{Total}}$
$\Xi^- + {}^{12}_6\text{C} \rightarrow {}^7_{\Lambda}\text{Li} + {}^4\text{He} + \Lambda^0 + \text{n}$	2.31	> 10.25	< -7.94
$\Xi^- + {}^{12}_6\text{C} \rightarrow {}^9_{\Lambda}\text{Be} + \text{d} + \Lambda^0 + \text{n}$	1.89	> 9.98	< -8.10
$\Xi^- + {}^{12}_6\text{C} \rightarrow {}^{10}_{\Lambda}\text{Be} + \text{p} + \Lambda^0 + \text{n}$	3.72	> 11.14	< -7.42
$\Xi^- + {}^{13}_6\text{C} \rightarrow {}^8_{\Lambda}\text{Li} + {}^4\text{He} + \Lambda^0 + \text{n}$	5.84	> 10.34	< -4.49
$\Xi^- + {}^{13}_6\text{C} \rightarrow {}^9_{\Lambda}\text{Be} + \text{t} + \Lambda^0 + \text{n}$	3.19	> 9.72	< -6.53
$\Xi^- + {}^{13}_6\text{C} \rightarrow {}^{10}_{\Lambda}\text{Be} + \text{d} + \Lambda^0 + \text{n}$	1.00	> 10.54	< -9.54
$\Xi^- + {}^{14}_7\text{N} \rightarrow {}^9_{\Lambda}\text{Be} + {}^4\text{He} + \Lambda^0 + \text{n}$	15.46	> 12.55	< 2.90
$\Xi^- + {}^{14}_7\text{N} \rightarrow {}^{12}_{\Lambda}\text{B} + \text{p} + \Lambda^0 + \text{n}$	11.52	> 17.07	< -5.54
$\Xi^- + {}^{15}_7\text{N} \rightarrow {}^{10}_{\Lambda}\text{Be} + {}^4\text{He} + \Lambda^0 + \text{n}$	8.19	> 12.87	< -4.69
$\Xi^- + {}^{17}_8\text{O} \rightarrow {}^{12}_{\Lambda}\text{B} + {}^4\text{He} + \Lambda^0 + \text{n}$	12.72	> 16.71	< -4.07

Table 3 Some production reaction of single Λ hypernucleus with two neutron emission

Possible Production Reaction	Q-Value (MeV)	E_{total} (MeV)	B_{Ξ} (MeV) = $Q - E_{Total}$
$\Xi^- + {}^{12}_6C \rightarrow {}^6_{\Lambda}Li + {}^4He + \Lambda^0 + 2n$	-4.42	> 8.72	< -13.14
$\Xi^- + {}^{12}_6C \rightarrow {}^9_{\Lambda}Be + p + \Lambda^0 + 2n$	-0.35	> 8.26	< -8.61
$\Xi^- + {}^{13}_6C \rightarrow {}^8_{\Lambda}Li + {}^4He + \Lambda^0 + 2n$	-14.73	> 7.92	< -22.64
$\Xi^- + {}^{13}_6C \rightarrow {}^9_{\Lambda}Be + d + \Lambda^0 + 2n$	-3.06	> 7.97	< -11.03
$\Xi^- + {}^{13}_6C \rightarrow {}^{10}_{\Lambda}Be + p + \Lambda^0 + 2n$	-1.73	> 8.67	< -10.40
$\Xi^- + {}^{14}_7N \rightarrow {}^8_{\Lambda}Be + {}^4He + \Lambda^0 + 2n$	-3.31	> 10.36	< -13.67
$\Xi^- + {}^{14}_7N \rightarrow {}^{11}_{\Lambda}B + p + \Lambda^0 + 2n$	-1.06	> 12.35	< -13.41
$\Xi^- + {}^{15}_7N \rightarrow {}^{12}_{\Lambda}B + p + \Lambda^0 + 2n$	0.69	> 12.97	< -12.28
$\Xi^- + {}^{17}_8O \rightarrow {}^{11}_{\Lambda}B + {}^4He + \Lambda^0 + 2n$	0.13	> 13.28	< -13.15
$\Xi^- + {}^{18}_8O \rightarrow {}^{12}_{\Lambda}B + {}^4He + \Lambda^0 + 2n$	4.67	> 13.68	< -9.10

Table 4 Some production reaction of single Λ hypernucleus with three neutron emission

Possible Production Reaction	Q-value (MeV)	E_{total} (MeV)	B_{Ξ} (MeV) = $Q - E_{Total}$
$\Xi^- + {}^{13}_6C \rightarrow {}^6_{\Lambda}Li + {}^4He + \Lambda^0 + 3n$	-9.37	> 7.96	< -17.33
$\Xi^- + {}^{13}_6C \rightarrow {}^9_{\Lambda}Be + p + \Lambda^0 + 3n$	-5.29	> 7.08	< -12.36
$\Xi^- + {}^{14}_7N \rightarrow {}^7_{\Lambda}Be + {}^4He + \Lambda^0 + 3n$	-15.67	> 9.24	< -24.91
$\Xi^- + {}^{14}_7N \rightarrow {}^{10}_{\Lambda}B + p + \Lambda^0 + 3n$	-10.85	> 9.89	< -20.73
$\Xi^- + {}^{15}_7N \rightarrow {}^8_{\Lambda}Be + {}^4He + \Lambda^0 + 3n$	-14.15	> 9.37	< -23.53
$\Xi^- + {}^{15}_7N \rightarrow {}^9_{\Lambda}Be + {}^3He + \Lambda^0 + 3n$	-15.95	> 8.96	< -24.91
$\Xi^- + {}^{15}_7N \rightarrow {}^{11}_{\Lambda}B + {}^4He + \Lambda^0 + 3n$	-11.89	> 10.36	< -22.25
$\Xi^- + {}^{17}_8O \rightarrow {}^{10}_{\Lambda}B + {}^4He + \Lambda^0 + 3n$	-9.65	> 11.47	< -21.13
$\Xi^- + {}^{17}_8O \rightarrow {}^{13}_{\Lambda}C + p + \Lambda^0 + 3n$	0.70	> 14.47	< -13.77
$\Xi^- + {}^{17}_8O \rightarrow {}^{10}_{\Lambda}B + {}^4He + \Lambda^0 + 3n$	-7.91	> 11.77	< -19.67

Secondly, the single Λ hypernucleus (track#1) was identified from its decay point B. The particle species of decay daughters, track#3 and #4 are assigned and considered all the possible decay modes of the single Λ hypernucleus. The Q values for decay modes are obtained and compared with the total kinetic energy of track #3 and #4. All decay modes of the single Λ hypernucleus (track #1) at vertex point B were shown in Table (5a) and Table (5b).

We also checked the angle between two tracks, track #3 and track #4. Take the coordinates of two points, vertex A and end point of each track, we obtained the vector of each track. The angle between two tracks emitted from vertex B is defined as

$$\theta = \cos^{-1}(\vec{v}_3 \cdot \vec{v}_4) \quad (2)$$

where θ is the angle between track #3 and #4. Its value was $133.7 \pm 4.5^\circ$. That angle value was less than 180° , it pointed out that another neutral particle could be emitted from vertex B according to conservation of momentum. Among them, the most possible decay mode of the single Λ

hypernucleus is non-mesonic decay with neutron emission. Only Lamba Beryllium 10 was found to be acceptable for track #1 candidate.

Table 5 (a) Some decay modes of single lambda hypernucleus track #1

Decay mode	Q-value (MeV)	E _{total} (MeV)	Q - E _{Total} (MeV)
${}^4_{\Lambda}\text{He} \rightarrow p + p + 2n$	166.01	> 77.34	< 77.36
${}^5_{\Lambda}\text{He} \rightarrow p + p + 3n$	144.70	> 69.79	< 74.91
${}^5_{\Lambda}\text{He} \rightarrow p + d + 2n$	146.92	> 137.86	< 9.07
${}^5_{\Lambda}\text{He} \rightarrow d + p + 2n$	146.92	> 75.41	< 71.41
${}^5_{\Lambda}\text{He} \rightarrow {}^3_2\text{He} + \pi^- + 3n$	34.72	> 29.85	< 4.87
${}^6_{\Lambda}\text{He} \rightarrow p + d + 3n$	146.60	> 116.72	< 29.87
${}^6_{\Lambda}\text{He} \rightarrow d + p + 3n$	146.60	> 68.57	< 78.02
${}^6_{\Lambda}\text{He} \rightarrow d + d + 2n$	148.82	> 134.19	< 14.63
${}^6_{\Lambda}\text{Li} \rightarrow {}^3_2\text{He} + p + 3n$	153.00	> 73.14	< 79.86
${}^7_{\Lambda}\text{He} \rightarrow {}^3_2\text{He} + p + 2n$	145.74	> 114.31	< 31.43
${}^7_{\Lambda}\text{He} \rightarrow t + p + 3n$	149.77	> 67.71	< 82.06
${}^7_{\Lambda}\text{He} \rightarrow t + d + 2n$	152.00	> 131.43	< 20.56
${}^7_{\Lambda}\text{Li} \rightarrow {}^3_2\text{He} + p + 2n$	146.26	> 67.77	< 78.48
${}^7_{\Lambda}\text{Li} \rightarrow {}^3_2\text{He} + d + 2n$	148.48	> 126.86	< 21.61
${}^7_{\Lambda}\text{Li} \rightarrow {}^4_2\text{He} + p + 2n$	166.84	> 72.40	< 94.44
${}^7_{\Lambda}\text{Li} \rightarrow {}^4_2\text{He} + d + 2n$	169.06	> 169.02	< 0.038
${}^8_{\Lambda}\text{He} \rightarrow t + d + 3n$	150.80	> 112.48	< 38.31
${}^8_{\Lambda}\text{Li} \rightarrow {}^3_2\text{He} + d + 3n$	140.01	> 110.05	< 29.96
${}^8_{\Lambda}\text{Li} \rightarrow {}^3_2\text{He} + d + 3n$	158.37	> 67.36	< 91.00
${}^8_{\Lambda}\text{Li} \rightarrow {}^4_2\text{He} + d + 2n$	160.59	> 124.16	< 36.43
${}^9_{\Lambda}\text{Li} \rightarrow {}^4_2\text{He} + d + 2n$	156.86	> 108.31	< 48.55
${}^9_{\Lambda}\text{Be} \rightarrow {}^6_3\text{Li} + p + 2n$	144.90	> 75.28	< 69.62
${}^{10}_{\Lambda}\text{Be} \rightarrow {}^6_3\text{Li} + p + 3n$	141.34	> 70.30	< 71.04

Table 5 (b) Some decay modes of single lambda hypernucleus track #1

Decay mode	Q value	E _{total}	Q - E _{Total}
$^{10}_{\Lambda}Be \rightarrow {}^6_3Li + d + 2n$	143.57	> 119.06	< 24.51
$^{10}_{\Lambda}Be \rightarrow {}^7_3Li + p + 2n$	148.59	> 76.33	< 72.26
$^{10}_{\Lambda}Li \rightarrow {}^4_2He + t + 3n$	158.13	> 152.49	< 5.65
$^{11}_{\Lambda}Be \rightarrow {}^6_3Li + d + 3n$	137.15	> 105.86	< 31.30
$^{11}_{\Lambda}Be \rightarrow {}^7_3Li + p + 3n$	142.17	> 71.06	< 71.14
$^{11}_{\Lambda}Be \rightarrow {}^7_3Li + d + 2n$	144.40	> 118.21	< 26.18
$^{12}_{\Lambda}B \rightarrow {}^7_3Li + p + 2n$	146.71	> 87.51	< 59.19
$^{12}_{\Lambda}Be \rightarrow {}^7_3Li + d + 3n$	143.27	> 105.33	< 37.93
$^{13}_{\Lambda}C \rightarrow {}^9_5B + p + 3n$	128.58	> 87.33	< 41.25
$^{13}_{\Lambda}C \rightarrow {}^9_5B + d + 2n$	130.81	> 126.57	< 4.23
$^{13}_{\Lambda}B \rightarrow {}^9_4Be + p + 3n$	142.22	> 79.62	< 62.00
$^{13}_{\Lambda}B \rightarrow {}^9_4Be + d + 3n$	144.45	> 121.03	< 23.42
$^{14}_{\Lambda}C \rightarrow {}^{10}_5B + p + 3n$	131.59	> 90.19	< 41.39
$^{14}_{\Lambda}C \rightarrow {}^{10}_5B + d + 2n$	133.81	> 128.60	< 5.21
$^{14}_{\Lambda}B \rightarrow {}^9_4Be + d + 3n$	138.44	> 108.29	< 30.15
$^{14}_{\Lambda}N \rightarrow {}^{12}_6C + p + 2n$	150.03	> 125.53	< 24.49
$^{15}_{\Lambda}C \rightarrow {}^{10}_5B + d + 3n$	124.65	> 114.47	< 10.17
$^{16}_{\Lambda}N \rightarrow {}^{12}_6C + p + 3n$	139.02	> 107.50	< 31.52
$^{16}_{\Lambda}N \rightarrow {}^{13}_6C + p + 2n$	143.97	> 131.44	< 12.53
$^{17}_{\Lambda}N \rightarrow {}^{12}_6C + d + 3n$	138.05	> 126.02	< 12.03
$^{17}_{\Lambda}N \rightarrow {}^{13}_6C + p + 3n$	140.78	> 111.54	< 29.23
$^{17}_{\Lambda}N \rightarrow {}^{14}_6C + p + 2n$	148.95	> 137.36	< 11.59
$^{18}_{\Lambda}N \rightarrow {}^{13}_6C + d + 3n$	136.66	> 128.70	< 7.84
$^{18}_{\Lambda}N \rightarrow {}^{14}_6C + p + 3n$	142.50	> 115.59	< 26.91
$^{18}_{\Lambda}N \rightarrow {}^{15}_6C + p + 2n$	143.72	> 143.33	< 0.388

Results and Discussions

Results of Range and Angle Measurement of Tracks in Single Λ Hypernucleus Event

Ranges and angles of all the tracks in single Λ hypernucleus event were measured by using the microscope system under constant temperature and humidity. We obtained the range and angles from measured coordinates at the vertex and click points on the track. The measured lengths and emission angles of those tracks were expressed in Table (6).

Table 6 Range and angles of all the tracks in single- Λ hypernucleus event

Vertex	Track Number	Range (μm)	θ (Degree)	ϕ (Degree)
A	#1	3.3 ± 0.2	108.4 ± 3.6	292.3 ± 13.1
	#2	15.5 ± 0.4	122.9 ± 3.8	104.8 ± 3.6
B	#3	14.1 ± 0.8	158.3 ± 3.3	48.7 ± 12.2
	#4	11111.1 ± 5.9	67.9 ± 3.1	233.1 ± 0.5

Results of Determination of Density and Shrinkage factor of Nuclear Emulsion Plate

In event analysis, kinetic energies of charged particles were obtained from their ranges. Kinetic energy of particles, ranges and density of the medium was related to each other. We used the thorium decay series in nuclear emulsion as range- energy relation calibration source. We measured the coordinates of alpha tracks emitted from ^{212}Po in thorium decay series. The coordinates (x, y, z) at the end points of the tracks were measured by using the overall viewer. From measured coordinates, $\Delta x^2 + \Delta y^2$ and Δz^2 were obtained. We plotted the scattered graphs, Δz^2 versus $\Delta x^2 + \Delta y^2$ graphs for ^{212}Po . The plotted data are fitted with straight line.

The range of alpha particles emitted from ^{212}Po and shrinkage factor of nuclear emulsion plate were obtained by fitting the straight line equation with scattered plotted graphs. Its values were $49.87 \pm 0.22 \mu\text{m}$ and 2.2 ± 0.01 , respectively.

By changing the density of nuclear emulsion plate in energy- range relation, we produced a corresponding range of alpha particles for average kinetic energy of α particles from ^{212}Po of 8.785 MeV. Densities of nuclear emulsion plate of sheet #5, Module #26 was $3.59 \pm 0.02 \text{ gcm}^{-3}$. That density value was used when we obtained the kinetic energy of the charge particle track which were included in Single Λ hypernucleus event.

Results of Event Reconstruction

We constructed the single Λ hypernucleus event which was found in plate #5 of Mod# 26 of JPARC E07 Experiment. Firstly, we consider at the production point of the single Λ hypernucleus. We considered as Ξ^- hyperon was absorbed by a light nucleus (C, N, and O) in nuclear emulsion at the point A. We obtained the kinetic energy of charged particles were obtained from their ranges. The kinetic energy of neutral particles was obtained from momentum balance. We assigned the particle species which were emitted from point A and obtained the Q values for each production mode. Results were shown in the 2nd column of Table (7). The total kinetic energy (E_{Total}) which includes kinetic energy of charged and uncharged particles were obtained. The results were shown in the 3rd column of Table (7). The binding energy of Ξ^- hyperon was obtained from the difference between the Q value and E_{Total} . The corresponding binding energies were presented in the 4th column of Table (7). For the production modes with negative Q value and large values of B_{Ξ^-} were rejected. The most acceptable production mode of single lambda hypernucleus and binding energy of Ξ^- hyperon in $^{14}_7\text{N}$ nucleus were $\Xi^- + ^{14}_7\text{N} \rightarrow ^{10}_\Lambda\text{Be} + ^4\text{He} + \Lambda^0$ and $0.51 \pm 0.17 \text{ MeV}$, respectively. On the other hand, we considered at the decay point of the single Λ hypernucleus event at point B.

Table 7 Possible production reaction of single Λ hypernucleus

Possible Production Reaction	Q-value (MeV)	E_{total} (MeV)	B_{Ξ^-} (MeV) = $Q - E_{Total}$	Comments
$\Xi^- + {}^{14}_7N \rightarrow {}^{10}_{\Lambda}Be + {}^4He + \Lambda^0$	19.01	18.51 ± 0.17	0.51 ± 0.17	acceptable
$\Xi^- + {}^{12}_6C \rightarrow {}^8_{\Lambda}Li + {}^4He + \Lambda^0$	10.78	14.4 ± 0.14	-3.66 ± 0.14	rejected
$\Xi^- + {}^{12}_6C \rightarrow {}^7_{\Lambda}Li + {}^4He + \Lambda^0 + n$	2.31	10.25 ± 0.14	-7.94 ± 0.01	rejected
$\Xi^- + {}^{12}_6C \rightarrow {}^9_{\Lambda}Be + d + \Lambda^0 + n$	1.89	9.979 ± 0.17	-8.10 ± 0.17	rejected
$\Xi^- + {}^{12}_6C \rightarrow {}^6_{\Lambda}Li + {}^4He + \Lambda^0 + 2n$	-4.42	8.72 ± 0.14	-13.14 ± 0.14	rejected
$\Xi^- + {}^{12}_6C \rightarrow {}^9_{\Lambda}Be + p + \Lambda^0 + 2n$	-0.35	8.26 ± 0.17	-8.61 ± 0.17	rejected
$\Xi^- + {}^{16}_8O \rightarrow {}^{12}_{\Lambda}B + {}^4He + \Lambda^0$	16.86	25.07 ± 0.22	-8.21 ± 0.22	rejected

Possible decay modes of the single Λ hypernucleus (track #1) are expressed in Table (8). Possible decay mode, Q value, E_{Total} , difference of Q value and E_{Total} and comment are described in that Table. According to collinear checking between track #3 and track #4, we can concluded that neutron(s) will be emitted at point B. By comparing with production mode and decay modes, possible decay mode of single lambda hypernucleus is ${}^{10}_{\Lambda}Be \rightarrow {}^6_3Li + d + 2n$. The type of hypernucleus was lambda beryllium 10 hypernucleus.

Table 8 Possible decay modes of the single Λ hypernucleus

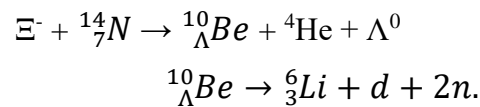
Decay mode	Q value	E_{total}	$Q - E_{Total}$	Comments
${}^4_{\Lambda}He \rightarrow p + p + 2n$	166.01	> 77.34	< 77.36	rejected
${}^5_{\Lambda}He \rightarrow p + p + 3n$	144.70	> 69.79	< 74.91	rejected
${}^5_{\Lambda}He \rightarrow p + d + 2n$	146.92	> 137.86	< 9.07	rejected
${}^5_{\Lambda}He \rightarrow d + p + 2n$	146.92	> 75.41	< 71.41	rejected
${}^5_{\Lambda}He \rightarrow {}^3_2He + \pi^- + 3n$	34.7	> 29.85	< 4.87	rejected
${}^6_{\Lambda}He \rightarrow p + d + 3n$	146.60	> 116.72	< 29.87	rejected
${}^6_{\Lambda}He \rightarrow d + p + 3n$	146.60	> 68.57	< 78.02	rejected
${}^6_{\Lambda}He \rightarrow d + d + 2n$	148.82	> 134.19	< 14.63	rejected
${}^6_{\Lambda}Li \rightarrow {}^3_2He + p + 3n$	153.00	> 73.14	< 79.86	rejected
${}^7_{\Lambda}He \rightarrow t + d + 2n$	152.00	> 131.43	< 20.56	rejected
${}^7_{\Lambda}Li \rightarrow {}^3_2He + p + 2n$	146.26	> 67.77	< 78.48	rejected
${}^8_{\Lambda}He \rightarrow t + d + 3n$	150.80	> 112.48	< 38.31	rejected
${}^8_{\Lambda}Li \rightarrow {}^3_2He + d + 3n$	140.01	> 110.05	< 29.96	rejected
${}^9_{\Lambda}Li \rightarrow {}^4_2He + d + 2n$	156.86	> 108.31	< 48.55	rejected
${}^9_{\Lambda}Be \rightarrow {}^6_3Li + p + 2n$	144.90	> 75.28	< 69.62	rejected
${}^{10}_{\Lambda}Be \rightarrow {}^6_3Li + p + 3n$	141.34	> 70.30	< 71.04	rejected
${}^{10}_{\Lambda}Be \rightarrow {}^6_3Li + d + 2n$	143.57	> 119.06	< 24.51	accepted
${}^{11}_{\Lambda}Be \rightarrow {}^6_3Li + d + 3n$	137.15	> 105.86	< 31.30	rejected
${}^{11}_{\Lambda}Be \rightarrow {}^7_3Li + p + 3n$	142.17	> 71.06	< 71.14	rejected
${}^{12}_{\Lambda}B \rightarrow {}^7_3Li + p + 2n$	146.71	> 87.51	< 59.19	rejected
${}^{12}_{\Lambda}Be \rightarrow {}^7_3Li + d + 3n$	143.27	> 105.33	< 37.93	rejected
${}^{13}_{\Lambda}C \rightarrow {}^9_5B + p + 3n$	128.58	> 87.33	< 41.25	rejected
${}^{16}_{\Lambda}N \rightarrow {}^{12}_6C + p + 3n$	139.02	> 107.50	< 31.52	rejected

Discussions

We checked and choose suitable events among many single Λ hypernucleus events to analyze. We have analyzed one of the single Λ hypernucleus events found in the upper layer of emulsion plate #5 of Module #26. We measured the range and angles of all the tracks in single Λ hypernucleus event in temperature and humidity controlled room by using the microscope system. Since the kinetic energies of charged particles were obtained from their ranges and range-energy of the particle depends on the density of material medium. Therefore, we made range energy relation calibration by using α particles tracks, emitted from ^{212}Po in Thorium decay series. The density of emulsion plate which detected our analyzed event was $3.59 \pm 0.02 \text{ gcm}^{-3}$. When we obtained kinetic energy of each charged particle in the event from its range, that density value was used. Event reconstruction in the emulsion was based on the conservation laws of energy and momentum. Firstly, we considered at the production point of single Λ hypernucleus event point A. All possible production reactions were considered and obtained. Q value for each production mode was obtained with known mass of hypernucleus. The total kinetic energy of particles was also obtained. By comparing with the Q value and total kinetic energy, the most possible production was estimated. A Ξ^- hyperon was captured by nitrogen nucleus and decayed into lambda beryllium 10 hypernucleus, helium and one Λ hyperon were emitted, $\Xi^- + {}^{14}_7\text{N} \rightarrow {}^{10}_\Lambda\text{Be} + {}^4\text{He} + \Lambda^0$. On the other hand, we considered at the point B, decay point of the single Λ hypernucleus event with the same manner as considering in production mode. The angle between track #3 and #4, which were the decay daughters of the single Λ hypernucleus, were checked. Its angle value was $135 \pm 4.5^\circ$. It shows that another neutral particle such as neutron(s) can be emitted from point B. We estimated the decay mode of the single Λ hypernucleus was lambda beryllium 10 hypernucleus decay into lithium 6, deuteron and two neutrons were emitted, ${}^{10}_\Lambda\text{Be} \rightarrow {}^6_3\text{Li} + d + 2n$.

Conclusion

We have analyzed a single Λ hypernucleus which was found in the J-PARC E07 experiment based on the conservation laws of energy and momentum. The type of hypernucleus was beryllium 10 hypernucleus and the production and decay modes of the event were,



Moreover, the binding energy of Ξ^- hyperon in nitrogen nucleus was $0.51 \pm 0.17 \text{ MeV}$.

Acknowledgements

Our gratitude to Rectors and Pro-rectors from University of Mandalay and Yadanabon University. We would like to thank Professor Dr Lei Lei Win, Head of Department of Physics, Professor Dr Kalyar Thwe, Professor Dr Nyein Wint Lwin, Professor Dr Nay Win Oo, Department of Physics, University of Mandalay for their kind encouragement to carry out research work.

References

- Aoki. S., *et al.*, (1991), Prog. Theor. Phys. 85, 951–956.
- Ahn. J. K. *et al.*, (2001), Phys. Rev. Lett. 87, 132504.
- Bando. H, *et.al*, (1990), Intl. J. Mod. Phys.**A**, **5**, 4023.
- Dover.C. B, *et.al*, (1991), Phys. Rev. C44 1905
- Davis, D. H., (2005), Nucl. Phys. A **754**, 3c.
- Dalitz R. H, *et al.*, (1989), Proc. Roy. Soc. Lond. A **426**, 1
- Danysz. M, *et al.*, (1963), Nucl. Phys. **49**, 121.
- Hiyama. E and K. Nakazawa, (2018), Annu. Rev. Nucl. Part. Sci. **68**, 13159.
- Imai. K, *et.al* J-PARC E07 Proposal
- Khaustov. P. *et al.*, Phys. Rev. C61 (2000) 054603.
- Mondal, A. S. *et.al*, (1975), Nuov. Cim. A **28**, 42.
- Myo. A. M. M, (2019), M. Sc Thesis, Yadanabon University.
- Takahashi. H, *et al.*, (2001), Phys. Rev. Lett. **87**, 212502.
- Tint. K. T. (2017), Myingyan Deg. Col. Res. J, 8,1, 90-97.
- Yoshida. J, Nakazawa. K and Umehara. K, (2014), JPS Conf. Proc. **1**, 013070..